pressible laminar flow in rectangular ducts," J. Appl. Mech. **27**, 403 (1960).

[7] Singh, S. N., "Heat transfer in viscous incompressible fluids," Ph.d. Thesis, Indian Institute of Technology, Kharagupur, India (1957).

[8] Singh, S. N. and Nigam, S. D., "Heat transfer by laminar flow between parallel plates under the action of transverse magnetic field," Quart. J. Math. Appl. Mech. XIII, 85–98 (1960).

[9] Hartmann, J., "Hg-dynamics I, theory of the laminar flow of an electrically conducting liquid in a homogeneous magnetic field," Kgl. Danske Videnskab. Setskab Mat. Fys. Medd. **15** (1937).

[10] Chang, C. C. and Yen, J. T., "Magneto-hydrodynamic channel flow as influenced by wall conductance," Z. Angew. Math. Phys. XIII, 3 (1962).

[11] Whittaker, E. T. and Watson, G. N., *Modern Analysis* (Cambridge University Press, England, 1927), p. 36.

[12] Singh, S. N., "The determination of eigen-functions of a certain Sturm-Liouville equation and its application to problems of heat transfer," Appl. Sci. Res. **7**, 237–250 (1958).

NOVEMBER 1964 AIAA JOURNAL VOL. 2, NO. 11

Hypersonic Viscous Flow Near the Stagnation Streamline of a Blunt Body: I. A Test of Local Similarity

HSIAO C. KAO*
Stanford University, Stanford, Calif.

The flow near the stagnation streamline of a blunt body is often analyzed by using the approximation of local similarity, which reduces the equations of motion to a system of ordinary differential equations. This scheme is equivalent to truncating at one term a power-series expansion of the flow variables from the stagnation point, neglecting backward influence. The accuracy of such a truncation is examined in this paper. The principal assumption is that the Navier-Stokes equations are valid. In addition, it is assumed that the validity of the first truncation can be evaluated by comparing it with the second. The conclusion is that the usual assumption of local similarity is remarkably accurate for predicting flow quantities near the stagnation streamline.

Nomenclature

C'	=	$(\bar{h}_{1s}/\bar{U}_\infty^2)^{1/2}$, constant proportionality for viscosity law
h	=	$\bar{h}/\bar{U}_\infty^2$, dimensionless enthalpy
$\bar{k}$	=	coefficient of heat conductivity
M_∞	=	freestream Mach number
p	=	$\bar{p}/\bar{\rho}_\infty\bar{U}_\infty^2$, dimensionless pressure
Pr	=	$C_p\bar{\mu}/\bar{k}$, Prandtl number
r	=	$\bar{r}/\bar{R}_b$, dimensionless radial distance
$\bar{R}_b$	=	body radius
R_e	=	$\bar{\rho}_\infty\bar{U}_\infty\bar{R}_b/\bar{\mu}_{1s}$, Reynolds number
u	=	$\bar{u}/\bar{U}_\infty$, dimensionless tangential velocity component
$\bar{U}_\infty$	=	freestream velocity
v	=	$\bar{v}/\bar{U}_\infty$, dimensionless normal velocity component
γ	=	adiabatic exponent
θ	=	angle between r and axis of symmetry
μ	=	$\bar{\mu}/\bar{\mu}_{1s}$, dimensionless viscosity coefficient
ρ	=	$\bar{\rho}/\bar{\rho}_\infty$, dimensionless density

Subscripts

b	=	body condition
s	=	conditions immediately behind shock wave
1, 2, . . .	=	order of expansion in powers of $\sin\theta$
∞	=	freestream conditions

Superscripts

$(\bar{\ })$	=	physical quantities

I.1 Introduction

THE problem of determining the flow field behind a detached shock wave is a very difficult one, especially when viscosity is taken into account. However, if we limit ourselves to predicting the flow properties near the stagnation streamline of a blunt body, an approximate local analysis may be made by utilizing the concept of local similarity. This consists in assuming that the variables are separable, except for some terms that are negligible in a thin shock layer. Then the Navier-Stokes equations reduce to a system of ordinary differential equations.

Local similarity can be imbedded in a systematic scheme of successive approximations by expanding the flow quantities in powers of the distance from the stagnation point [see Eqs. (9)]. Substituting the expansions into the equations of motion and equating terms that contain like powers of the distance yield a system of ordinary differential equations. The first-order equations, obtained by equating terms that contain the lowest power of the distance, consist mostly of first-order terms [quantities with subscript 1 in Eqs. (9)], and a few second-order ones (quantities with subscript 2). This can be seen, for example, in Eqs. (10–13). A similar situation exists in any higher-order equations. Hence, the number of equations is always less than the number of dependent variables. In order to overcome this difficulty, we use a so-called truncation scheme. That is, we truncate the expansions in such a way that the number of equations becomes equal to the number of the dependent variables, so that the equations are solvable. The first truncation consists of the set of first-order equations without some of the second-order quantities. The actual procedure of truncating the equations

Presented as Preprint 63-437 at the AIAA Conference on Physics of Entry into Planetary Atmospheres, Cambridge, Mass., August 26–28, 1963; revision received August 3, 1964. This work was supported by the Air Force Office of Scientific Research Contract No. AF49(638)-965 and Grant No. AFOSR-96-63. The writer is greatly indebted to M. Van Dyke of Stanford University for his suggestion of this study, his guidance, and encouragement.

* Research Assistant, Department of Aeronautics and Astronautics; now at Norair Division, Northrop Corporation, Hawthorne, Calif.

needs explanation and will be described later. The next step in improving the accuracy is to include the second-order terms in the first-order equations. In order that these second-order terms be determinable, we must also consider the second-order equations simultaneously with the first-order equations. Since the second-order equations contain a few third-order terms, we must also truncate them to insure that the number of equations is again equal to the number of dependent variables. Although we need an infinite number of truncations to determine the problem exactly, the approximation can be expected to improve continuously as the order of the truncation increases, especially if our interest is limited to the vicinity of the stagnation streamline.

The presence of additional terms whose order is higher than that of the equations in which they appear is a symptom of backward influence, associated with the elliptic nature of the governing equations in the subsonic region.

As pointed out by Hayes and Probstein, for a spherical or cylindrical body, the functional form of the solution with local similarity is analogous to that of the solution having full cylindrical or spherical symmetry.[1] If the shock layer is thin and the discontinuous shock wave is nearly concentric with the body, the assumption of cylindrical or spherical symmetry is a good approximation, and it has been applied successfully by Lighthill and others.[4, 9] The first truncation in the present scheme corresponds to cylindrical or spherical symmetry and hence is equivalent to the assumption of local similarity. Thus, examining the accuracy of the first truncation is equivalent to examining the validity of local similarity.

Since all previous authors have assumed local similarity (see for example, Refs. 2-9), it is important to know its accuracy. This is the purpose of the present investigation.

If we simply delete all second-order terms from the first-order equations to reduce the number of the dependent variables to the number of equations available, an anomaly will occur, because we neglect so many terms that no well-behaved solution can exist under the given boundary conditions. This can be seen in Swigart's inviscid calculation of the first truncation for a given spherical shock.[11] There the standoff distance cannot be determined since nowhere in the field do the flow quantities satisfy the tangency condition on the body. For this reason, the present truncation is an indented one [see Eqs. (9)]; that is, in each truncation one more term is retained in the expansion for the pressure than for the other flow quantities. This pattern is suggested by Lighthill's solution for constant-density flow between a sphere and a concentric spherical shock wave.[4] His flow variables have just the form of our first truncation. Our first truncation is also essentially the same as the locally similar solutions proposed in Ref. 1, without some of the small terms.

To test the accuracy of the first truncation, we consider the flow near the axis of symmetry, i.e., the stagnation streamline for an unyawed body, ahead of an axisymmetric body (Fig. 1). The flow is assumed to be governed by the Navier-Stokes equations for an ideal gas with constant adiabatic exponent, constant Prandtl number, and zero bulk viscosity. The procedure is to calculate several numerical examples from the first and second truncations. If the changes from the first to second truncation are negligible, the first truncation is assumed to be accurate. This is an indirect verification, but we shall be content with it, since it is not possible here to find a rigorous proof for the accuracy of this truncation scheme.

In general, we calculate the numerical examples by applying the Navier-Stokes equations to the entire shock layer, assuming that the shock wave is discontinuous.[1] This is the so-called viscous-layer approximation. However, when the Reynolds number is small, viscous effects also prevail upstream, the shock layer can no longer be regarded as thin compared with the body radius, and the shock wave is not a discontinuity. Consequently, we must consider the flow field

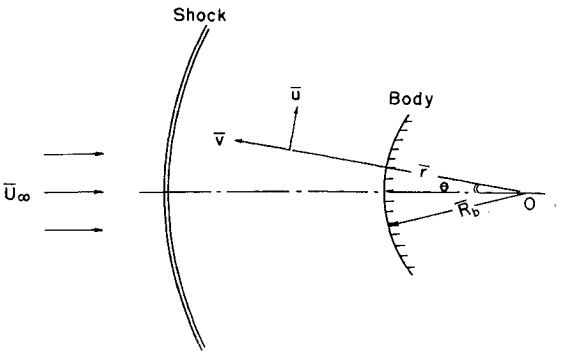

Fig. 1 Coordinate system.

of a single continuous region, without imposing the shock conditions between the freestream and the body surface. In this case, we integrate the equations for the first truncation directly from the freestream conditions to the body surface, or vice versa.

Ho and Probstein[2] and others have carried out calculations based on the viscous-layer approximation for a somewhat limited range of Reynolds numbers using a system of equations slightly different from the first truncation. A small but seemingly useful innovation is made here, so that the numerical integration is less laborious and more stable even for high Reynolds numbers. Levinsky and Yoshihara[3] have integrated a system of equations similar to those of Ho and Probstein without the viscous-layer approximation. However, viscous-layer theory will be emphasized in this study, because it is simpler and is believed to give the essential features when the Reynolds number is not too small. The extent to which the viscous-layer approximation fails is beyond the scope of the present study, but will be considered in Part II.

All numerical calculations have been carried out with $M_\infty = 10$, $Pr = 0.7$, and $\gamma = \frac{11}{9}$. These conditions are almost the same as those used by Ho and Probstein. Hence, some of the first-truncation results bear a close resemblance to theirs.

Our results indicate that the usual assumption of local similarity can satisfactorily predict the flow properties near the stagnation streamline. However, if the Reynolds number is very small (say $R_e \leq 10$), it may be necessary to modify that conclusion. This matter is currently being investigated.

I.2 Basic Equations and Boundary Conditions

Spherical polar coordinates are used. They are illustrated in Fig. 1, together with the velocity components. Flow quantities are made dimensionless by dividing by the freestream conditions, as shown in the Nomenclature. The Reynolds number used here is of a mixed type, $R_e = \bar{\rho}_\infty \bar{U}_\infty R_b / \bar{\mu}_{1s}$, where $\bar{\mu}_{1s}$ denotes the coefficient of viscosity on the axis of symmetry immediately behind the shock wave. If there is no clearly defined shock wave in the flow, this is a fictitious quantity determined from the Rankine-Hugoniot relations.

The equations of motion for the dimensionless variables are

$$r\frac{\partial(\rho v)}{\partial r} + \frac{\partial(\rho u)}{\partial \theta} + \rho(2v + u\cot\theta) = 0 \tag{1}$$

$$\frac{1}{r}\frac{\partial p}{\partial \theta} + \rho\left(v\frac{\partial u}{\partial r} + \frac{u}{r}\frac{\partial u}{\partial \theta} + \frac{uv}{r}\right) = \frac{1}{R_e}\frac{1}{r^2}\frac{\partial}{\partial \theta}\times$$
$$\left[\frac{4\mu}{3}\left(\frac{\partial u}{\partial \theta} + v\right) - \frac{2\mu}{3}\left(r\frac{\partial v}{\partial r} + v + u\cot\theta\right)\right] + \frac{1}{R_e}\frac{\partial}{\partial r}\times$$
$$\left[\mu r\frac{\partial}{\partial r}\left(\frac{u}{r}\right) + \frac{\mu}{r}\frac{\partial v}{\partial \theta}\right] + \frac{1}{R_e}\frac{3\mu}{r}\left[r\frac{\partial}{\partial r}\left(\frac{u}{r}\right) + \frac{1}{r}\frac{\partial v}{\partial \theta}\right] +$$
$$\frac{1}{R_e}\frac{2\mu}{r^2}\left(\frac{\partial u}{\partial \theta} - u\cot\theta\right)\cot\theta \tag{2}$$

$$\frac{\partial p}{\partial r} + \rho\left(v\frac{\partial v}{\partial r} + \frac{u}{r}\frac{\partial v}{\partial \theta} - \frac{u^2}{r}\right) = \frac{1}{R_e}\frac{\partial}{\partial r}\left[\frac{4\mu}{3}\frac{\partial v}{\partial r} - \frac{2\mu}{3r}\left(\frac{\partial u}{\partial \theta} + 2v + u\cot\theta\right)\right] + \frac{1}{R_e}\frac{1}{r}\frac{\partial}{\partial \theta}\left[\mu r\frac{\partial}{\partial r}\left(\frac{u}{r}\right) + \frac{\mu}{r}\frac{\partial v}{\partial \theta}\right] + \frac{1}{R_e}\frac{4\mu}{r}\left(\frac{\partial v}{\partial r} - \frac{v}{r}\right) - \frac{1}{R_e}\frac{\mu}{r^2}\left[2\frac{\partial u}{\partial \theta} + 2u\cot\theta - r^2\frac{\partial}{\partial r}\left(\frac{u}{r}\right)\cot\theta - \frac{\partial v}{\partial \theta}\cot\theta\right] \quad (3)$$

$$\rho\left(v\frac{\partial h}{\partial r} + \frac{u}{r}\frac{\partial h}{\partial \theta}\right) = v\frac{\partial p}{\partial r} + \frac{u}{r}\frac{\partial p}{\partial \theta} + \frac{1}{R_e}\mu\left\{2\left(\frac{\partial v}{\partial r}\right)^2 + \frac{2}{r^2}\times\left(\frac{\partial u}{\partial \theta} + v\right)^2 + \frac{2}{r^2}(v + u\cot\theta)^2 + \left[r\frac{\partial}{\partial r}\left(\frac{u}{r}\right) + \frac{1}{r}\frac{\partial v}{\partial \theta}\right]^2\right\} - \frac{1}{R_e}\frac{2\mu}{3r^2}\left(r\frac{\partial v}{\partial r} + \frac{\partial u}{\partial \theta} + 2v + u\cot\theta\right)^2 + \frac{1}{R_e}\frac{1}{rPr}\left[\frac{\partial}{\partial \theta}\left(\frac{\mu}{r}\frac{\partial h}{\partial \theta}\right) + \frac{\partial}{\partial r}\left(\mu r\frac{\partial h}{\partial r}\right) + \mu\left(\frac{\partial h}{\partial r} + \frac{\cot\theta}{r}\frac{\partial h}{\partial \theta}\right)\right] \quad (4)$$

$$p = \frac{\gamma - 1}{\gamma}\rho h \quad (5)$$

$$\mu \sim h^{1/2} \quad (6)$$

These are, respectively, the equations of continuity, tangential momentum, normal momentum, energy, state, and viscosity.

For integration in the viscous-layer regime, the shock wave is assumed to be a sphere with the origin of the coordinate system at its center. Hence, the body obtained from the second truncation is axisymmetric but not necessarily a sphere. Its shape is determined by the given boundary conditions. The osculating sphere tangent to the body at the stagnation point is concentric with the shock wave. For direct integration through the shock wave, the body is always taken to be a sphere.

The fluid is assumed not to slip to the wall. Hence, the boundary conditions for the velocity components at the body surface are $u_b = v_b = 0$. For a "cold-wall" problem as here, this no-slip condition can be justified.

In regard to the outer boundary conditions, they differ with the methods undertaken. For viscous-layer approximation, the Rankine-Hugoniot relations are the outer boundary conditions. They are

$$\begin{aligned} p_s &= \frac{2\gamma M_\infty^2(1 - \sin^2\theta) - (\gamma - 1)}{\gamma(\gamma + 1)M_\infty^2} \\ u_s &= \sin\theta \\ v_s &= -\frac{\cos\theta}{\gamma + 1}\left[\gamma - 1 + \frac{2}{M_\infty^2(1 - \sin^2\theta)}\right] \\ h_s &= \frac{[2\gamma M_\infty^2(1 - \sin^2\theta) - (\gamma - 1)]\,[M_\infty^2(\gamma - 1)(1 - \sin^2\theta) + 2]}{M_\infty^4(\gamma - 1)(\gamma + 1)^2(1 - \sin^2\theta)} \end{aligned} \quad (7)$$

For direct integration through the shock wave, the free-stream conditions are then the outer boundary conditions. They are

$$p_\infty = \frac{1}{\gamma M_\infty^2} \qquad u_\infty = \sin\theta \qquad v_\infty = -\cos\theta \qquad h_\infty = \frac{1}{(\gamma - 1)M_\infty^2} \quad (8)$$

I.3 Expansion Scheme

The flow variables are expanded about the axis of symmetry with respect to $\sin\theta$ as follows:

$$\begin{aligned} p(r,\theta) &\sim p_1(r) + p_2(r)\sin^2\theta + p_3(r)\sin^4\theta + \ldots, \\ u(r,\theta) &\sim u_1(r)\sin\theta + u_2(r)\sin^3\theta + \ldots, \\ v(r,\theta) &\sim -v_1(r)\cos\theta - v_2(r)\cos\theta\sin^2\theta + \ldots, \\ h(r,\theta) &\sim h_1(r) + h_2(r)\sin^2\theta + \ldots, \\ \mu(r,\theta) &\sim \mu_1(r) + \mu_2(r)\sin^2\theta + \ldots, \end{aligned} \quad (9)$$

First truncation | Second truncation

Assuming that the coefficients in the series expansions and their derivatives are of order unity, substituting these into the equations of motion, and equating like powers of $\sin\theta$, we obtain the first set of equations. They are Eqs. (10–16) minus Eq. (14) with the terms enclosed by $\langle\ \rangle$ included. However, if we take the first truncation of the expansions, the terms in $\langle\ \rangle$ do not appear. They are written here for visualization and for use in the second truncation. Equation (14) is taken essentially from the second set of equations. It must be included, because the p_2 term is included in the first truncation:

$$p_1' = p_1\left[\frac{h_1'}{h_1} + \frac{1}{v_1}\left(\frac{2u_1}{r} - v_1'\right) - \frac{2}{r}\right] \quad (10)$$

$$u_1'' = \left(\frac{8}{3r} + \frac{h_1'}{2h_1} + R_e\frac{\rho_1 u_1}{\mu_1}\right)\frac{u_1 - v_1}{r} - R_e\frac{\rho_1 u_1' v_1}{\mu_1} - \frac{v_1'}{3r} - \left(\frac{2}{r} + \frac{h_1'}{2h_1}\right)u_1' + R_e\frac{2p_2}{r\mu_1} + \left\langle\frac{2v_2'}{3r} + \frac{v_2 h_1'}{rh_1} - \frac{16(2u_2 - v_2)}{3r} - \frac{2h_2}{3rh_1}\left(\frac{u_1 - v_1}{r} + v_1'\right)\right\rangle \quad (11)$$

$$v_1'' = -R_e\frac{3}{4\mu_1}(p_1' + \rho_1 v_1 v_1') - \left(\frac{2}{r} + \frac{h_1'}{2h_1}\right)v_1' + \frac{u_1'}{2r} - \left(\frac{7}{2r} + \frac{h_1'}{2h_1}\right)\frac{u_1 - v_1}{r} - \left\langle\frac{3v_2}{r^2}\right\rangle \quad (12)$$

$$h_1'' = R_e\frac{Pr}{\mu_1}(v_1 p_1' - \rho_1 v_1 h_1') - \frac{4Pr\,v_1'^2}{3} - \left(\frac{2}{r} + \frac{h_1'}{2h_1}\right)h_1' - \frac{4Pr}{3}\left(\frac{u_1 - v_1}{r} + 2v_1'\right)\frac{u_1 - v_1}{r} - \left\langle\frac{4h_2}{r^2}\right\rangle \quad (13)$$

$$p_2' = -p_1' + \frac{\rho_1 u_1}{r}(u_1 - v_1) \quad (14)$$

$$\rho_1 = [\gamma/(\gamma - 1)](p_1/h_1) \quad (15)$$

$$\mu_1 = C' h_1^{1/2} \quad (16)$$

Here the prime refers to differentiation with respect to r.

Similar equations can be obtained for the next set of equations. They are more complicated, the equation for tangential momentum being

$$u_2'' = -R_e\frac{\rho_1}{\mu_1}\left(u_2'v_1 + u_1'v_2 + \frac{u_1 v_2 + u_2 v_1 - 4u_1 u_2}{r}\right) - R_e\frac{p_2}{r\mu_1} + R_e\frac{1}{\mu_1}\left(\rho_2 - \frac{\rho_1}{2}\right)\left(-u_1'v_1 + u_1\frac{u_1 - v_1}{r}\right) +$$

Eq. (17) continued on next page

$$\frac{1}{r}\left(2v_2' + 5\frac{2u_2 - v_2}{r}\right) + 2\frac{\mu_2}{\mu_1}\left(\frac{v_1'}{r} + \frac{u_1 - v_1}{r^2}\right) + 6\frac{u_2 - v_2}{r^2} - \frac{\mu_1'}{\mu_1}\left(u_2' - \frac{u_2 - 3v_2}{r}\right) - \frac{2u_2' + 3v_2'}{r} - \frac{\mu_2'}{\mu_1}\left(u_1' - \frac{u_1 - v_1}{r}\right) - \frac{\mu_2}{\mu_1}\left(u_1'' + \frac{2u_1' + v_1'}{r} - 2\frac{u_1 - v_1}{r^2}\right) + R_e\frac{4p_3}{r\mu_1} + \left\langle \frac{4\mu_1'v_3}{r\mu_1} + \frac{4v_3'}{3r} - \frac{32(3u_3 - v_3)}{3r^2} - \frac{8\mu_3}{3r\mu_1}\left(v_1' + \frac{u_1 - v_1}{r}\right)\right\rangle + \left\langle \frac{2\mu_2'v_2}{r\mu_1} - \frac{\mu_2}{\mu_1}\left(\frac{52u_2 - 20v_2}{3r^2} + \frac{2v_2'}{3r}\right)\right\rangle \quad (17)$$

The equations for the second truncation are Eqs. (10–13) with the terms in $\langle\ \rangle$ included, Eqs. (15) and (16) plus Eq. (17) and the other equations in the system excluding the terms enclosed by $\langle\ \rangle$. These terms are again written here to give an idea of the number of terms that are truncated. Note that, besides the terms with subscript 3, a few nonlinear secondary terms in Eq. (17) and the other equations in the system have also been neglected. This was done to make all the secondary equations strictly linear, which facilitates the numerical computations.

After substituting Eqs. (9) into Eqs. (7), (8), and the surface conditions, we can obtain the boundary conditions for the first and second truncations. The exterior boundary conditions are easily written and are not shown here. The surface conditions are given as follows:

First Truncation:

$$u_1(r) = 0 \qquad v_1(r) = 0 \qquad h_1(r) = 0.029$$
$$v_1'(r) = 0 \qquad \text{at} \qquad r = 1 \quad (18)$$

where $r = 1$ refers to the body radius at the stagnation point, h_1 at the surface is arbitrarily chosen as 0.029, which is approximately $\frac{1}{15}$ of the stagnation enthalpy, and the condition $v_1' = 0$ is imposed to ensure a finite pressure gradient at the surface.[9]

Second Truncation:

If the body is chosen as a sphere, and the surface temperature is constant, the surface conditions are

$$u_2(1) = 0 \qquad v_2(1) = 0 \qquad h_2(1) = 0 \qquad v_2'(1) = 0 \quad (19)$$

For an inverse problem, where the shock shape is prescribed and the body shape is to be determined in the course of solution, the surface conditions are

$$u_2(1) = -\eta_2 u_1'(1) \qquad v_2(1) = 0$$
$$h_2(1) = -\eta_2 h_1'(1) \qquad v_2'(1) = 4u_2(1) \quad (20)$$

Here the surface temperature is again assumed to be constant everywhere to second order, and η_2 is the second coefficient of the body radius r_b in the expansion

$$r_b = 1 + \eta_2 \sin^2\theta + \ldots,$$

with the origin at the origin of the coordinate system. There is one more boundary condition for the first truncation of the viscous-layer theory than is needed for solving the governing equations, and there are two more for the second truncation of the same method. The reason is that the location of the boundary is unknown. Instead of prescribing the surface temperature as constant, we can prescribe the body shape r_b and obtain the surface temperature when we solve the equations. In this case, $h_2(1)$ in Eq. (19) or (20) need not be of the form as shown; it can, in fact, be an arbitrary constant. In general, the body shape for an inverse problem in viscous flow depends upon the prescription of temperature on the body surface and, in contrast to the situation for inviscid flow, is not a unique quantity.

I.4 Calculation Procedures

Before carrying out any numerical integrations, we rewrite Eqs. (10–13) in the following form in order to introduce a simplification later and to stabilize the numerical computations:

$$\frac{v_1}{p_1^2}p_1'^2 + \left(R_e\frac{3}{4\mu_1} - \frac{v_1'}{p_1} + R_e\frac{Prv_1^2}{h_1\mu_1}\right)p_1' = AA - \frac{v_1}{h_1}BB - \frac{2}{r}(u_1' - v_1') + \frac{2}{r^2}(u_1 - v_1) + \frac{h_1'}{h_1}\left(v_1' - \frac{v_1h_1'}{h_1}\right) + \frac{v_1p_1''}{p_1} \quad (21)$$

$$u_1'' = \text{same as Eq. (11)} \quad (22)$$

$$v_1'' = AA - R_e(3p_1'/4\mu_1) \quad (23)$$

$$h_1'' = BB + R_e(Prv_1p_1'/\mu_1) \quad (24)$$

where

$$AA = -R_e\frac{3}{4\mu_1}\rho_1v_1v_1' - \left(\frac{2}{r} + \frac{h_1'}{2h_1}\right)v_1' + \frac{u_1'}{2r} - \left(\frac{7}{r} + \frac{h_1'}{h_1}\right)\frac{u_1 - v_1}{2r} - \left\langle\frac{3v_2}{r}\right\rangle \quad (25)$$

$$BB = -R_e\frac{Pr}{\mu_1}\rho_1v_1h_1' - \frac{4Prv_1'^2}{3} - \left(\frac{2}{r} + \frac{h_1'}{2h_1}\right)h_1' - \frac{4Pr}{3}\left(\frac{u_1 - v_1}{r} + 2v_1'\right)\frac{u_1 - v_1}{r} - \left\langle\frac{4h_2}{r^2}\right\rangle \quad (26)$$

Equation (21) is quadratic in p_1' and is obtained by differentiating Eq. (10) once with respect to r and substituting from Eqs. (12) and (13) for v_1'' and h_1''. One of its roots gives the pressure variation p_1'.

Thus far, no approximation has been introduced. In Eq. (21), however, p_1'' is not calculable in this arrangement. Thus it will be replaced by the expression for inviscid flow,

$$p_1'' = \frac{d}{dr}\left\{\frac{2\gamma p_1v_1(u_1 - v_1)}{r[v_1^2 - \gamma C^{1/\gamma}p_1^{1-1/\gamma}]}\right\} \quad (27)$$

where $C = p_{1s}/\rho_{1s}^{\gamma}$. This then contributes the only error in the recasting process. If there exists a definable boundary layer in the shock layer, such a replacement of p_1'' is exact outside the boundary layer and is approximately correct within the boundary layer, since the viscosity has only a third-order effect on the pressure variation at the stagnation point.[10] Thus, this error is expected to decrease as the Reynolds number increases. The real justification should, however, come from the numerical integration. It can be demonstrated that, for the case of $R_e = 100$, the error incurred is approximately 2%, which is regarded here as within tolerance. However, when the Reynolds number is so small that the boundary layer merges with the shock wave, this simplification is no longer applicable. Therefore we use the original system of Eqs. (10–16) for $R_e = 10$; in this case as well as in all low-Reynolds number cases, direct integration from the shock wave to the body surface can conveniently be carried out without encountering numerical instability.

In general, the last term on the right-hand side of Eq. (21) (the only term in the system that involves p_1'') is small in the shock layer compared with other terms. This is especially true near the body surface, since p_1'' is never large in the entire shock layer and v_1 is roughly one order of magnitude smaller than u_1 (because v_1' must also approach zero near the surface). Hence, under ordinary circumstances, Eqs. (21–27) can be used as a starting procedure if we initiate the integration from the surface, or as a terminal procedure if we initiate the integration from the shock wave. By following the latter procedure, we can avoid the complications of extrapolating the flow quantities to the surface. This frequently causes embarrassing errors; for instance, the equation of state in Ref. 2 is not satisfied at the surface. The other quantities are, however, believed to be correct.

Table 1 Flow quantities and their derivatives at shock and body for $R_e = 10$ calculated by viscous-layer approximation

	u_{1s}'	v_{1s}'	h_{1s}'	u_{2s}'	v_{2s}'	h_{2s}'	Standoff distance
First truncation	8.08	0.291	3.75	...	...	...	0.0718
Second truncation	8.04	0.245	3.78	−2.04	−0.669	−5.69	0.0720
	u_{1b}'	h_{1b}'	h_{1b}	u_{2b}'	h_{2b}'	h_{2b}	
First truncation	53.6	27.6	0.025	...	...	...	...
Second truncation	52.4	27.3	0.026	261	147	−0.281	...

The foregoing simplification can equally well be applied to the calculation of the second truncation. The expressions equivalent to Eq. (27) are rather complicated and will not be shown here.

The method of numerical integration employed herein is to reduce a two-point boundary-value problem to an initial-value problem with some unknown initial conditions that are to be guessed first and improved successively until the solutions converge to the specified boundary conditions at the opposite end. For the most part, the numerical computations were carried out on a Burroughs 220 electronic computing machine by use of a fourth-order Adams predictor-corrector method with the fourth-order Runge-Kutta method as a starting procedure. An automatic error-control procedure, which chose an optimum step size for the error tolerance specified, was imbedded in the program. The machine time for an individual run was between 10 and 30 min. Because of this relatively long running time, the accuracy of the results has been sacrificed, only three significant figures being given in Table 1. A few examples were, however, carried out with higher accuracy for the sole purpose of comparison.

The secondary equations, i.e., Eq. (17) and the other members in the system, are essentially linear except for a few nonlinear terms. In addition to the third-order terms, these nonlinear terms are neglected in the calculation of the second truncation so that superposition is feasible. It can be demonstrated that, if they are included, the final result does not show any significant change. The calculation procedure for the second truncation is as follows. First, we integrate the secondary equations with all the required boundary conditions satisfied by means of superposition in which the coefficients (i.e., the first-order quantities in these equations) are furnished by the calculations of the first truncation. Next, we include the coupling terms [i.e., the terms enclosed by $\langle\ \rangle$ in Eqs. (10–16)] and reintegrate the linearized equations of the second truncation. Now the boundary conditions at the two ends generally cannot be all satisfied, since the equations of the first truncation and the secondary equations were calculated individually without the coupling terms. Hence in general, a second or third cycle of integration is needed until all the boundary conditions are fulfilled. This time the coupling terms are to be retained with the approximate value given by the first-cycle calculation.

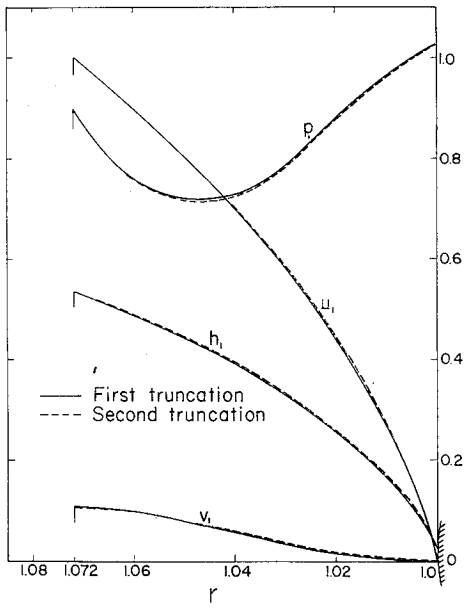

Fig. 2 Comparison of first truncation vs second truncation of viscous-layer approximation, $R_e = 10$.

I.5 Numerical Examples and Discussion

Examples were calculated with Reynolds numbers of 10, 100, and 1000 for the purpose of evaluating the accuracy of the first truncation. The range is wide enough to extend from the near free-molecule-flow to the regime of Prandt's boundary-layer theory. Discussion of this point will be given in Part II. It is therefore felt that the finding here is applicable to this problem regardless of the Reynolds number as long as a Navier-Stokes model is valid.

Examples for the First Truncation

For the cases of $R_e = 100$ and 1000, integrations were initiated at the body surface and carried to the shock wave using the simplified equations (21–27) plus Eqs. (14–16). For the flow at $R_e = 10$, integration was initiated at the shock wave and carried to the body surface using the complete equations (10–16) of the first truncation. In addition to these examples using viscous-layer approximation, computations were also made by integration through the shock wave. Results are not shown here but will be given in Part II.

Examples for the Second Truncation

The viscous-layer approximation is used here to check the accuracy of the first truncation. For the flow at $R_e = 10$, the integration is initiated at the shock wave, whose shape is chosen to be a sphere to the second order. The linearized equations of the second truncation are used, except that when the integration is sufficiently close to the surface the simplified equations are used as a terminal procedure. The alternative method for dealing with the boundary conditions of the second truncation is used. Thus the body shape is set as a sphere. The surface temperature is then a parameter obtained in the course of the calculation and varies with distance from the stagnation point. For the flow at $R_e = 100$, the integration is initiated on the surface with the simplified equations. The shock wave is still chosen as a sphere. Again the alternative method is employed for dealing with the boundary conditions. Two different body shapes have been considered: $r_b = 1$ and $r_b = 1 - 0.0087 \sin^2\theta$.

Without actually completing the numerical computation, we soon find that the modification of the first truncation due to the calculation of the second truncation is largest when the Reynolds number is smallest. This point can be visual-

ized by imagining Eqs. (10–16) reduced to Prandtl's boundary-layer equations, these being strictly of parabolic type so that the coupling terms do not appear. Hence, for flows with high Reynolds numbers where the boundary-layer approximation is valid, no backward influence can be present within the boundary layer; the slight modification of the result due to the second truncation comes from the slight improvement of the inviscid solution at the body surface. The question of how the higher truncations affect the inviscid solutions has been investigated by Swigart.[11] From his conclusion and the fact that the first truncation here is roughly equivalent to his second truncation, we may foresee even without any computation that the second truncation will give only a small improvement. Hence, it follows that the calculations using local similarity with high Reynolds number are not subject to any significant modification in higher truncations. This argument holds for the flow with $R_e = 1000$ because it falls in the boundary-layer regime. Computations were actually made; however, no result is shown here for the effect is hardly discernible to the scale of the plot.

Even for a Reynolds number as low as 10, the modification of the second truncation is barely visible in the flow profiles shown in Fig. 2. For this reason, Table 1 is included to show numerical values at the boundaries. Again, because it is not possible to plot a diagram discernible to a proper scale, no flow profiles at $R_e = 100$ are given.

From the foregoing numerical examples and reasoning, we conclude that the usual assumption of local similarity is very good for the purpose of a local analysis to determine the flow properties near the stagnation streamline.

References

[1] Hayes, W. D. and Probstein, R. F., *Hypersonic Flow Theory* (Academic Press, New York, 1959), Chap. X, p. 375.

[2] Ho, H.-T. and Probstein, R. F., "The compressible viscous layer in rarefied hypersonic flow," *Rarefied Gas Dynamics*, edited by L. Talbot (Academic Press, New York, 1961), p. 525.

[3] Levinsky, E. S. and Yoshihara, H., "Rarefied hypersonic flow over a sphere," *Hypersonic Flow Research*, edited by F. R. Riddell (Academic Press, New York, 1962), p. 81.

[4] Lighthill, M. J., "Dynamics of a dissociating gas, Part I, Equilibrium flow," J. Fluid Mech. **2**, 1–32 (1957).

[5] Herring, T. K., "The boundary layer near the stagnation point in hypersonic flow past a sphere," J. Fluid Mech. **7**, 257–272 (1960).

[6] Cheng, H. K., "Hypersonic shock-layer theory of the stagnation region at low Reynolds number," *Proceedings of the Heat Transfer and Fluid Mechanics Institute* (Stanford University Press, Stanford, Calif., 1961), p. 161.

[7] Hoshizaki, H., "Shock-generated vorticity effects at low Reynolds numbers," Lockheed Aircraft Corp., Missiles and Space Div. Rept., LMSD-48381, Vol. 1, pp. 9–43 (1959).

[8] Ferri, A., Zakkay, V., and Ting, L., "Blunt body heat transfer at hypersonic speed and low Reynolds number," J. Aerospace Sci. **28**, 962–971 (1961).

[9] Probstein, R. F. and Kemp, N., "Viscous aerodynamic characteristics in hypersonic rarefied gas flow," J. Aerospace Sci. **27**, 174–192 (1960).

[10] Van Dyke, M., "Second-order compressible boundary-layer theory with application to blunt bodies in hypersonic flow," *ARS Progress in Astronautics and Rocketry: Hypersonic Flow Research*, edited by F. R. Riddell (Academic Press, New York, 1962), Vol. 7, pp. 37–76.

[11] Swigart, R. J., "A theory of asymmetric hypersonic blunt-body flows," AIAA J. **1**, 1034–1042 (1963).